American Journal of Pathology, Vol. 160, No. 6, June 2002

Animal Model

A Mouse Model of Hepatocellular Carcinoma

Ectopic Expression of Fibroblast Growth Factor 19 in Skeletal Muscle of Transgenic Mice

Katrina Nicholes,* Susan Guillet,* Elizabeth Tomlinson,† Kenneth Hillan,* Barbara Wright,* Gretchen D. Frantz,* Thinh A. Pham,* Lisa Dillard-Telm,* Siao Ping Tsai,‡ Jean-Philippe Stephan,‡ Jeremy Stinson,† Timothy Stewart,† and Dorothy M. French*

From the Departments of Pathology, Molecular Biology,† and Assay and Automation Technology,‡ Genentech Incorporated, South San Francisco, California*

Most mouse models of hepatocellular carcinoma have expressed growth factors and oncogenes under the control of a liver-specific promoter. In contrast, we describe here the formation of liver tumors in transgenic mice overexpressing human fibroblast growth factor 19 (FGF19) in skeletal muscle. FGF19 transgenic mice had elevated hepatic α-fetoprotein mRNA as early as 2 months of age, and hepatocellular carcinomas were evident by 10 months of age. Increased proliferation of pericentral hepatocytes was demonstrated by 5-bromo-2′-deoxyuridine incorporation in the FGF19 transgenic mice before tumor formation and in nontransgenic mice injected with recombinant FGF19 protein. Areas of small cell dysplasia were initially evident pericentrally, and dysplastic/neoplastic foci throughout the hepatic lobule were glutamine synthetase-positive, suggestive of a pericentral origin. Consistent with chronic activation of the Wingless/Wnt pathway, 44% of the hepatocellular tumors from FGF19 transgenic mice had nuclear staining for β-catenin. Sequencing of the tumor DNA encoding β-catenin revealed point mutations that resulted in amino acid substitutions. These findings suggest a previously unknown role for FGF19 in hepatocellular carcinomas. ***(Am J Pathol 2002, 160:2295–2307)***

Most of the fibroblast growth factor (FGF) family members regulate cell proliferation, migration, and differentiation during development and in response to injury.[1] Notably, several of the FGFs and their receptors are implicated in the development and progression of tumors. For example, FGF8 up-regulation is correlated with growth and invasiveness of human breast carcinomas[2–4] and FGF8 isoforms are up-regulated in human prostate cancer.[5–7] In addition, elevated circulating levels of FGF2 were demonstrated in patients with B-cell chronic lymphocytic leukemia and chronic myeloid leukemia.[8] Mouse models overexpressing FGFs further implicate FGF family members in the pathogenesis of cancer. Transgenic mice overexpressing FGF8 under control of the mouse mammary tumor virus promoter develop breast tumors,[9] and transgenic mice overexpressing FGF10 under the control of a lung-specific promoter form pulmonary adenomas.[10] Mutations or overexpression of FGF receptors have also been implicated in neoplastic transformation. Up-regulation of FGFR4 is described in mammary fibroadenomas,[11] FGFR3 is constitutively activated in multiple myeloma,[12] and activating mutations were identified in FGFR2 and FGFR3 from gastric and colorectal cancers.[13]

The role of FGF19 in cancer is unknown. FGF19 is a novel member of the FGF family with unique specificity for FGFR4.[14] Unlike other FGF family members, FGF19 has minimal mitogenic activity on fibroblasts *in vitro*. To understand the *in vivo* effects of FGF19, we generated transgenic mice overexpressing FGF19 in skeletal muscle. We describe here a unique model of hepatocellular carcinoma (HCC) that developed in FGF19 transgenic mice by 10 months of age.

Primary cancer of the liver, or HCC, is the third most frequent cause of death by cancer in the world.[15] Consistent with the observation that oncogenes, growth factors, or viral genes are frequently up-regulated in human HCC, it is not surprising that overexpression of these genes in the liver also causes HCC in transgenic mice. Transgenic mouse models of HCC previously described include overexpression of transforming growth factor-α

Accepted for publication March 11, 2002.

Address reprint requests to Dorothy M. French, Genentech, Inc., MS 72B, 1 DNA Way, South San Francisco, CA 94080. E-mail: dfrench@gene.com.

Table 1. Gross and Histologic Changes in the Liver from FGF19 Transgenics

Age (months)	Sex	Gross evidence of tumor	Dysplasia (basophilic foci)	Carcinoma	Age-matched wild-type mice*
2 to 4	F	0/17	0/17	0/17	10
	M	0/7	0/7	0/7	7
7 to 9	F	0/15	5/15 (33%)	0/15	14
	M	0/15	1/15 (7%)	0/15	14
10 to 12	F	8/10 (80%)	7/10 (70%)	8/10 (80%)	11
	M	2/9 (22%)	7/9 (77%)	2/9 (22%)	7

Incidence is expressed as number of animals with indicated parameter over the total number of animals in the group.
*Total numbers of age-matched wild-type mice are indicated in the last column although no dysplastic or neoplastic changes were found in this group.

(TGF-α) alone[16–19] or in combination with c-*myc*,[20] mutated H-ras,[21] hepatitis B viral genes encoding HbsAg and HBx,[22,23] and SV40 large T antigen.[24,25] Liver-specific promoters drive transgene expression in all of these models. To our knowledge, no mouse model has been described in which ectopic expression of an oncogene or growth factor leads to hepatic tumors.

In the normal liver, hepatocytes are mitotically quiescent but can readily proliferate in response to injury.[26] Several studies investigating the pathogenesis of HCCs reveal that constitutive hepatocellular proliferation is a prerequisite for transformation.[27] Hepatocellular proliferation leading to transformation may be initiated by inflammation. For example, transgenic mice overexpressing the hepatitis B virus large envelope protein develop focal hepatocellular necrosis because of excessive accumulation of protein within the endoplasmic reticulum, followed by inflammation that precedes tumor formation.[28,29] Inflammation is also prominent in mice lacking the *mdr2* gene that results in failure to transport phosphatidyl choline into the bile and inability to emulsify biliary components leading to inflammation, hepatocellular proliferation, and HCC by 18 months of age.[30] Similarly, mice lacking peroxisomal fatty acyl-CoA oxidase develop hepatitis followed by hepatocellular regeneration then hepatocellular tumors by 15 months of age.[31] Alternatively, in the absence of inflammation, increased hepatocellular proliferation and subsequent transformation can result from genomic alteration. For example, insertional activation of an oncogene leading to hepatocellular proliferation before HCC was demonstrated in woodchuck hepatitis virus infection. HCC in woodchucks results from integration of woodchuck hepatitis virus at the c-*myc* or *n-myc2* locus.[32–34] Tumor induction without preceding inflammation or necrosis also occurs in transgenic mice overexpressing TGF-α,[19,20,35,36] c-*myc*,[20] c-Ha-ras,[21] or SV40 large T antigen.[37,38]

The results of this study indicate that tumors arise from pericentral hepatocytes after increased proliferation and dysplasia. In addition, increased proliferation is accompanied by expression of α-fetoprotein (AFP), an oncofetal protein used as a marker for neoplastic transformation of hepatocytes,[39] before occurrence of tumors. Similar to mice overexpressing TGF-α and/or c-*myc*, early dysplastic foci are predominantly small-cell type in the FGF19 transgenic mice. In contrast, neither *c-myc* nor *tgf-α* mRNA was elevated in liver tumors from the FGF19 transgenic mice. Nuclear accumulation of β-catenin was evident in neoplastic cells from some of the FGF19 liver tumors suggesting nuclear translocation of β-catenin and activation of the Wingless/Wnt signaling pathway. This is the first report implicating an FGF family member in development of hepatocellular tumors and this model may provide insight into the pathogenesis of human HCC.

Materials and Methods

Generation of FGF19 Transgenic Mice

All animal protocols were approved by an Institutional Animal Care and Use Committee. Construction of the FGF19 transgenic mice was previously described.[40] Briefly, the human FGF19 cDNA[14] was ligated 3′ to the pRK splice donor/acceptor site that was preceded by the myosin light chain.[41] The FGF19 cDNA was also followed by the splice donor/acceptor sites present between the fourth and fifth exons of the human growth hormone gene.[42] The entire expression fragment was purified free from contaminating vector sequences and injected into one-cell mouse eggs derived from FVB $\times$ FVB matings. Transgenic mice were identified by polymerase chain reaction (PCR) analysis of DNA extracted from tail biopsies using DNeasy and PCR core kits (Qiagen, Valencia, CA). Expression of FGF19 was determined by real-time reverse transcriptase-PCR (TaqMan; Perkin Elmer, Emeryville, CA) on total RNA from skeletal muscle biopsies.

Gross and Histopathological Analyses

To determine the onset of liver changes in FGF19 transgenic mice, transgenic and wild-type mice were evaluated at designated intervals throughout the course of a year (Table 1). Five to eight each of male and female FGF19 transgenic mice and wild-type littermates were euthanized every month and evaluated as indicated below. Body and liver weights were recorded. Livers were examined for gross lesions. Specimens from each lobe and from grossly visible tumors were fixed in 10% buffered formalin, embedded in paraffin, sectioned at 4 μm, and used for immunohistochemistry, *in situ* hybridization, or stained with hematoxylin and eosin (H&E). For *in vivo* labeling of S-phase hepatocytes, 5-bromo-2′-deoxyuridine (BrdU; Sigma Chemical Co., St. Louis, MO) was dissolved in phosphate-buffered saline (PBS) by heating

at a concentration of 100 mg/ml. While still warm, BrdU solution was injected into osmotic minipumps (ALZET model 1002) and incubated in excess PBS for 4 hours in amber vials. Pumps were subcutaneously implanted between the shoulder blades and left implanted for 6 days. For molecular analysis, half of each tumor was quickly frozen in liquid nitrogen and stored at −80°C.

Measurement of Serum FGF19 Protein

Human FGF19 was measured in serum from transgenic mice using an enzyme-linked immunosorbent assay. The 96-well Nunc-Immunoplates (Nalge Nunc Intl. Corp., Rochester, NY) were coated at 4°C overnight with a mouse monoclonal antibody anti-rhFGF19 (mAb 1A6; Genentech, Inc., South San Francisco, CA) at 2 μg/ml in carbonate buffer (pH 9.6). Enzyme-linked immunosorbent assay plates were washed with PBS and 0.05% Tween-20 (pH 7.2) and blocked for 2 hours with PBS, 0.05% Tween-20, and 0.5% bovine serum albumin (pH 7.2). Serum samples and rhFGF19 standard were diluted in PBS, 0.5% bovine serum albumin, 0.2% bovine IgG, 0.25% CHAPS, 5 mmol/L ethylenediaminetetraacetic acid (pH 7.4), 0.05% Tween-20, and 0.35 mol/L NaCl and incubated on the enzyme-linked immunosorbent assay plate for 2 hours. After washing with PBS and 0.05% Tween-20 (pH 7.2), the enzyme-linked immunosorbent assay plates were incubated with a secondary biotinylated monoclonal anti-rhFGF19 (mAb 2A3, Genentech, Inc.) antibody for 1 hour before washing, followed by incubation with Amdex streptavidin-horseradish peroxidase (Amersham Pharmacia Biotech, Piscataway, NJ). Signal was revealed using the chromogenic substrate TMB (Kirkegaard & Perry Laboratories, Gaithersburg, MD) and read at 450/620 nm after addition of phosphoric acid (1 mol/L).

In Situ *Hybridization*

^{33}P-labeled murine FGFR4 and AFP riboprobes were used to evaluate gene expression in murine liver, lung, spleen, kidney, and brain. To generate the probes, PCR primers were designed to amplify either a 654-bp fragment of murine AFP spanning from nucleotides 731 to 1385 of NM_007423 (upper: 5′ CCTCCAGGCA ACAACCATTA T; lower, 5′ CCGGTGAGGT CGATCAG) or a 170-bp fragment of murine FGFR4 spanning from nucleotides 327 to 497 of NM_008011 (upper: 5′ CGAGTACGGGGTTGGAGA; lower: 5′ TGCTGAGTGTCTTGGGGTCTT). Primers included extensions encoding 27-nucleotide T7 or T3 RNA polymerase initiation sites to allow *in vitro* transcription of sense or anti-sense probes, respectively, from the amplified products.[43] Sections were deparaffinized, deproteinated in 4 μg/ml of proteinase K for 30 minutes at 37°C, and further processed for *in situ* hybridization as previously described.[44] ^{33}P-UTP labeled sense and anti-sense probes were hybridized to the sections at 55°C overnight. Unhybridized probe was removed by incubation in 20 μg/ml of RNase A for 30 minutes at 37°C, followed by a high stringency wash at 55°C in 0.1× standard saline citrate for 2 hours, and dehydration through graded ethanols. The slides were dipped in NBT2 nuclear track emulsion (Eastman Kodak, Rochester, NY), exposed in sealed plastic slide boxes containing desiccant for 4 weeks at 4°C, developed, and counterstained with H&E.

Immunohistochemical and Morphometric Analyses

Monoclonal antibodies to glutamine synthetase (Chemicon, Temecula, CA) and β-catenin (Transduction Laboratories, Lexington, KY) were prelabeled using the mouse-on-mouse Iso IHC Kit (InnoGenex, San Ramon, CA) following the manufacturer's instructions. Pretreatment of all slides included antigen retrieval in preheated DAKO Target Retrieval (DAKO, Carpinteria, CA) for 20 minutes at 99°C and endogenous peroxidase blocking by KPL Blocking Solution (Kirkegaard & Perry) for 4 minutes at room temperature. After PBS washing, the endogenous biotin was blocked using an Avidin Blocking Kit (Vector Laboratories, Burlingame, CA) and the endogenous proteins were blocked using Power Block Reagent (InnoGenex, San Ramon, CA). The sections were incubated with the prelabeled primary antibodies for 60 minutes at room temperature and washed in PBS. Sections were then labeled with Vectastain Elite avidin biotin complex (ABC)-peroxidase (Vector Laboratories) followed by tyramide amplification (NEN Life Science Products, Boston, MA) and visualization using metal enhanced diaminobenzidine (Pierce, Rockford, IL). Murine IgG (Oncogene, Cambridge, MA) was used as an isotype control; normal liver and cell pellets were used to determine tissue and antigen specificity.

Cellular proliferation was evaluated using a monoclonal antibody to BrdU (clone IU-4; Caltag Laboratories, Burlingame, CA). After deparaffinization, sections were treated with preheated 2 N HCl for 30 minutes at 37°C, rinsed with borate buffer (pH 7.6) for 1 minute, and digested in preheated 0.01% trypsin (Sigma) for 3 minutes at 37°C. Endogenous peroxidase and endogenous biotin were blocked as previously described. Endogenous proteins were blocked with 10% normal horse serum (Life Technologies, Inc., Rockville, MD) in 3% bovine serum albumin and PBS (Boehringer Mannheim, Indianapolis, IN) for 30 minutes. The sections were then incubated with anti-BrdU antibody for 60 minutes, followed by biotinylated horse anti-mouse IgG, Vectastain Elite ABC-Peroxidase (Vector Laboratories), then Immunopure metal-enhanced diaminobenzidine substrate (Pierce) for visualization. For morphometric analysis of BrdU-labeled sections, 1000 to 3000 hepatocytes were counted for each animal using MetaMorph image analysis software (Universal Imaging Corp., Downington, PA). The labeling index denotes the number of BrdU-positive hepatocytes divided by the total number of hepatocytes counted and indicated as a percentage.

Table 2. Primers and Probes Used for Real-Time Reverse Transcriptase-PCR Analysis of Growth Factors and Oncogenes

Gene name	Forward primer 5′-3′	Reverse primer 5′-3′	Probe 5′-3′
Murine RPL19	GCG CAT CCT CAT GGA GCA CA	GGT CAG CA GGA GCT TCT TG	CAC AAG CTG AAG GCA GAC AAG GCC C
Murine TGF-α	CAG CTT TAG TGT CCG AAC GGT	GTG TAC AGG CAC TGG GAT GGT	CCA GCC AGT CGC AGC AGC CA
Murine c-*myc*	AGC AAC AAC CGC AAG TGC T	GTC CGC CTC TTG TCG TTT TC	CAG CCC CAG GTC CTC AGA CAC GG
Murine AFP	GAA GTG GAT CAC ACC CGC TT	TTT TCG TGC AAT GCT TTG GA	CCT CAT CCT CCT GCT ACA TTT CGC TGC
Murine hepatocyte growth factor	CCT GAC ACC CCT TGG GAG T	GTT TCC ATA GGG ACA TCA GTC TCA T	TTG TGC AAT TAA AAC GTG CGC TCA CAG T
Murine FGFR4	CGG GAC TAG CTG CAA AAC T	TGA AGT CCC AAG GCC TCT A	TGC TCT AAA CAT TTC TAG TTC CCC CAA ACA

Gene Expression

Total RNA was extracted from frozen liver samples using RNA STAT-60 (Tel-test "B" Inc., Friendswood, TX). Liver samples were homogenized in the RNA STAT-60, incubated at room temperature for 5 minutes, and centrifuged at 12,000 $\times$ *g* for 10 minutes at 4°C. Chloroform was added to the supernatant to extract the RNA, followed by isopropanol precipitation for 10 minutes. The pellet was washed with 75% EtOH and resuspended in diethyl pyrocarbonate-treated water. Total RNA was DNase-treated followed by addition of DNase inactivation reagent (Ambion) and centrifugation. Supernatant was used as RNA template for real-time PCR. RNA concentration was determined using a spectrophotometer (DU 530; Beckman) and visualized on a 1.2% agarose gel.

Primers and probes were designed using Primer Express 1.1 (PE Applied Biosystems) for murine RPL19, FGFR4, TGF-α, hepatocyte growth factor, c-*myc*, and AFP (Table 2). Amplification reactions (50 μl) contained 100 ng of RNA template, 5 mmol/L of $MgCl_2$, 1$\times$ buffer A, 1.2 mmol/L of dNTPs, 2.5 U of TaqGold polymerase, 20 U of RNase inhibitor, 12.5 U of MuLV reverse transcriptase, 2 μmol/L each forward and reverse primer, and 5 μmol/L of probe (Perkin Elmer). Thermal cycle (Perkin Elmer ABI Prism 7700 sequence detector) conditions were 48°C for 30 minutes, 95°C for 10 minutes, and 95°C for 15 seconds, and 60°C for 1 minute for 40 cycles. Analyses of data were performed using Sequence Detector 1.6.3 (PE Applied Biosystems) and results for genes of interest were normalized to RPL19.

Recombinant FGF19 Protein

Recombinant human FGF19 (rFGF19) was expressed intracellularly in *Escherichia coli* as previously described.[40] The FGF19 protein was purified via anion exchange chromatography, size exclusion chromatography, and preparative reverse-phase chromatography. Sequence analysis and analysis by mass spectrometry indicated that purified rFGF19 had the expected mass and N-terminal sequence. Nontransgenic female FVB mice were injected intraperitoneally with 30 μg of rFGF19 protein or $ArgPO_4$ vehicle in a volume of 100 μl once daily for 6 days. BrdU was administered by Alzet minipumps placed subcutaneously on day 1, as described above, and the mice were necropsied on the day 6.

Cloning and Sequencing of β-Catenin

DNA extracted from tumor tissue was PCR-amplified using forward and reverse primers 5′ TAC AGG TAG CAT TTT CAG TTC AC 3′ and 5′ TAG CTT CCA AAC ACA AAT GC 3′, respectively. PCR products were subcloned into pCR2.1 using the TA cloning kit (Invitrogen, Carlsbad, CA). Sequencing of subcloned PCR products was done as outlined in the ABI Prism Big Dye Terminator Cycle Sequencing Ready Reaction Kit on an Applied Biosystems Prism 3700 DNA Analyzer. M13 primers were used for the TA vector. The trace files were edited and aligned using Sequencer (Gene Codes Corp., Ann Arbor, MI). Mutations were identified by comparing the trace files to the murine β-catenin sequence published in GenBank (NM_007614).

Statistical Analysis

Data are presented as the means plus or minus standard deviations. Comparisons between transgenic and wild-type mice or protein-injected and vehicle control mice were made using an unpaired Student's *t*-test.

Results

Hepatocellular Dysplasia and Neoplasia in FGF19 Transgenic Mice

As early as 2 to 4 months of age hepatocytes adjacent to central veins formed a single columnar row with nuclei polarized away from the endothelial basement membrane of the central vein (Figure 1A) that was not observed in wild-type mice (Figure 1B). Dysplastic changes (areas of altered hepatocellular foci) preceded tumor formation and were evident by 7 to 9 months (Table 1). Within this age group, 33% of female and 7% of male transgenics had hepatocellular dysplasia without evidence of neoplasia. Interestingly, dysplastic foci were predominantly of the small-cell type and oriented around central veins (Figure 1C). Rarely, foci of large dysplastic hepatocytes were noted (Figure 1D). FGF19 transgenic mice developed liver tumors by 10 to 12 months of age at an overall frequency of 53% (Table 1). Within the 10- to 12-month-old group, 80% (8 of 10) of female and 22% (2 of 9) of male FGF19 transgenic mice had locally invasive HCCs (Figure 2). Tumors were solitary or multifocal, involving different liver lobes. Mean

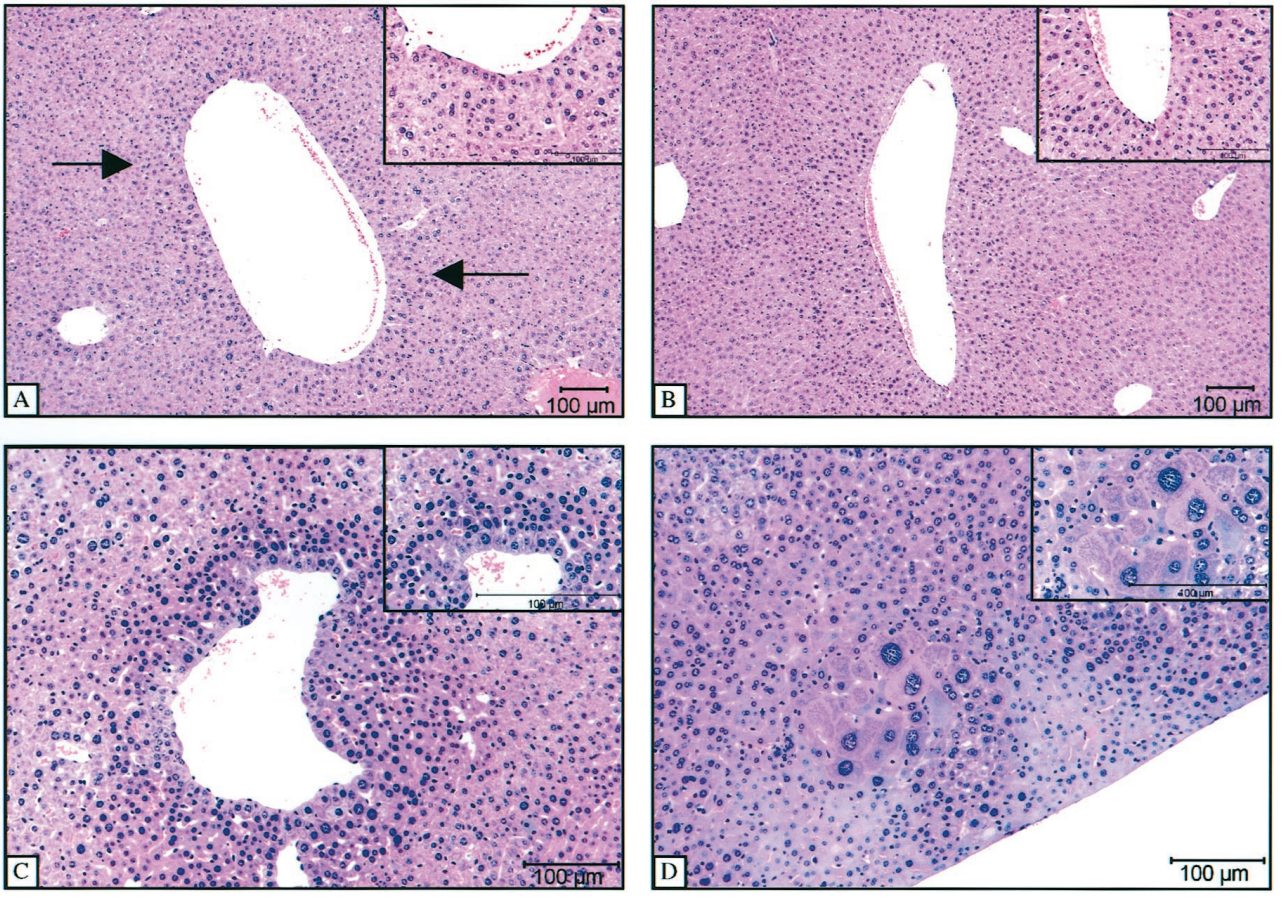

Figure 1. Preneoplastic hepatocellular changes in FGF19 transgenic mice. As early as 14 weeks of age pericentral hepatocytes formed a dense cluster around the central veins (**arrows**) with polarization of nuclei of the innermost hepatocytes away from the vessel lumen in FGF19 transgenics (**A**) that was not present in liver from nontransgenic littermate mice (**B**). Pericentral small dysplastic hepatocytes (**C**) were the predominant type of hepatocellular dysplasia although foci of large dysplastic hepatocytes (**D**) were occasionally noted. **Arrows** delineate areas of altered hepatocellular foci (shown at higher magnification in the **insets**). Original magnifications: ×100 (**A** and **B**); ×400 (**C** and **D**). **Inset** original magnifications: ×400 (**A** and **B**); ×600 (**C** and **D**).

liver weights in the 10- to 12-month-old female FGF19 transgenics were increased 30% relative to liver weights of wild-type mice (mean liver weight, 1.97 g and 1.54 g, respectively; $P < 0.01$) attributable to tumor mass. The mean liver weight for 10- to 12-month-old male FGF19 transgenic mice was not significantly different from wild-type mice, likely because of the low incidence of tumors in the male transgenic mice (mean liver weight, 1.53 g and 1.63 g, respectively; $P = 0.37$). Histologically, neoplastic hepatocytes invaded and replaced adjacent normal hepatic parenchyma (Figure 2B). HCCs in the FGF19 transgenic mice were predominantly the solid type although a trabecular pattern was occasionally noted. Figure 2C shows the typical morphology of neoplastic hepatocytes: neoplastic cells with nuclear pleomorphism and frequent mitoses (Figure 2C, arrows). The tumors did not metastasize. Other tissues evaluated histologically included: lungs, heart, spleen, kidneys, bone (femur), intestines, brain, pituitary gland, thyroid glands, and skeletal muscle. Despite the fact that FGF19 was expressed in the skeletal muscle, no histological changes were evident in that tissue.

Serum FGF19 protein levels were determined in the FGF19 transgenic and wild-type mice to assess whether phenotypic differences between male and female transgenic mice could be because of differences in levels of protein expression. The 2- to 4-month-old transgenic females ($n = 16$) have mean serum FGF19 protein levels of 77.7 ng/ml and the transgenic males in the same age group ($n = 7$) have mean serum FGF19 protein levels of 63.2 ng/ml ($P = 0.07$). FGF19 serum protein levels are considerably lower in the older animals. The 7- to 9-month-old transgenic females ($n = 10$) have mean serum FGF19 protein levels of 21.8 ng/ml and transgenic males in the same age group ($n = 13$) have mean serum FGF19 protein levels of 18.6 ng/ml ($P = 0.20$). The 10- to 12-month-old transgenic females ($n = 9$) have mean FGF19 serum protein levels of 24.3 ng/ml and the transgenic males in the same age group have mean FGF19 serum protein levels of 20.7 ng/ml ($P = 0.41$).

FGFR4, the Receptor for FGF19, Is Expressed in Murine Liver

FGF19 was previously shown to selectively bind with high affinity to FGFR4.[14] Although FGFR4 expression has been

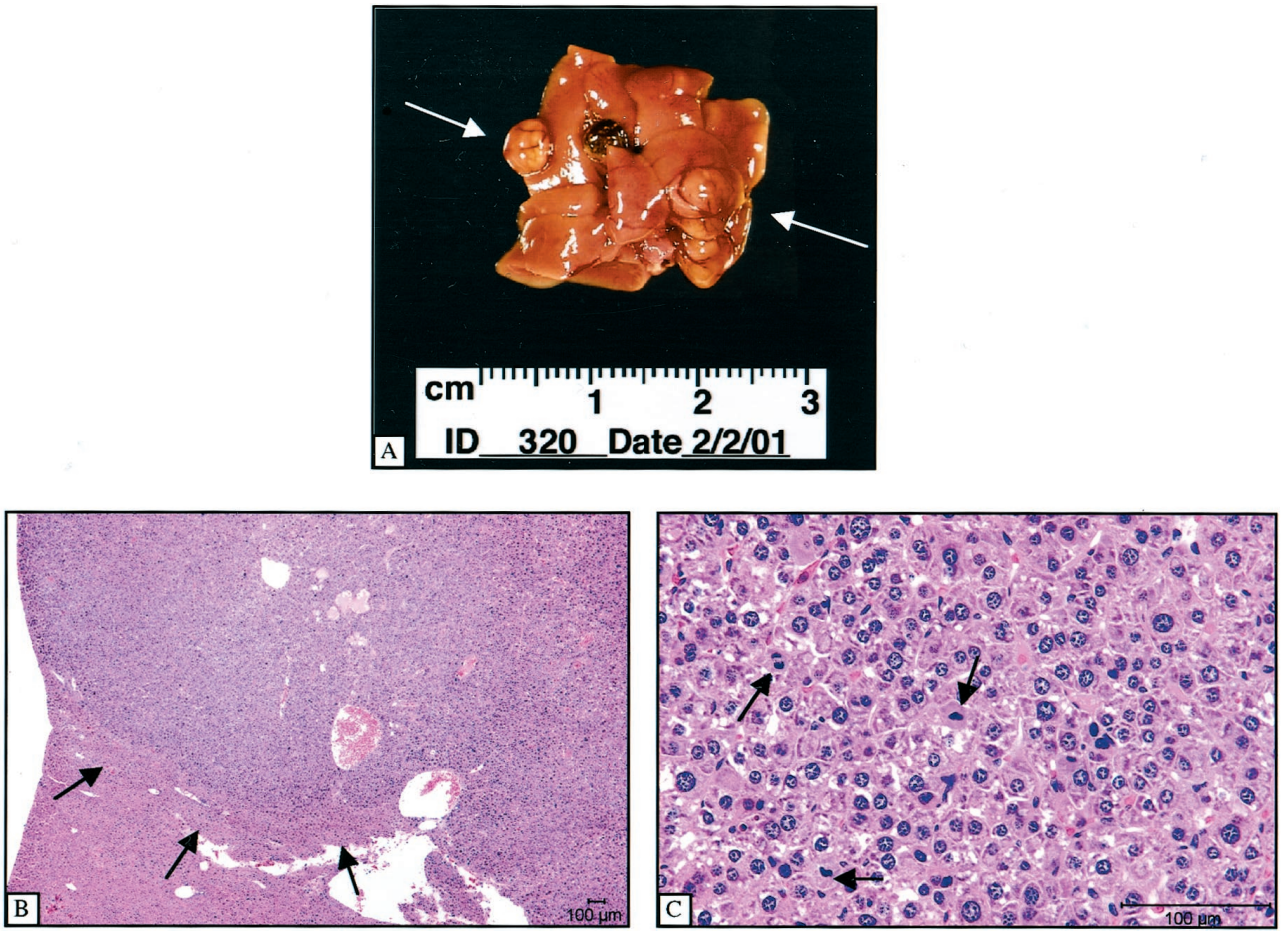

Figure 2. Hepatocellular neoplasia in FGF19 transgenic mice. **A:** Multiple, large, raised tumors protrude from the hepatic surface of the liver from a 10-month-old FGF19 transgenic mouse (**arrows**). **B:** Histologically, neoplastic cells invade and replace normal hepatic architecture and are arranged in solid sheets or cords. **Arrows** mark the border of the tumor and adjacent normal liver. **C:** Pleomorphism of neoplastic hepatocytes and atypical mitotic figures (**arrows**). Original magnifications: ×40 (**B**); ×400 (**C**).

demonstrated in mouse and rat hepatocytes,[45–47] we used *in situ* hybridization with a ^{33}P-labeled murine FGFR4 riboprobe to determine expression patterns in wild-type and FGF19 transgenic mice. In both wild-type and FGF19 transgenic mice, a strong signal for murine *fgfr4* mRNA was present in hepatocytes adjacent to central veins and in random, small hepatocytes throughout the lobule (Figure 3). There was not a significant difference in signal intensity or distribution based on genotype. In addition, real-time reverse transcriptase-PCR did not demonstrate any difference in levels of *fgfr4* mRNA between FGF19 transgenic and wild-type mice (data not shown).

FGF19 Transgenic Mice and rFGF19 Protein-Injected Mice Showed Increased Hepatocellular Proliferation

Constitutive hepatocellular proliferation is considered a prerequisite for neoplastic transformation.[27] Therefore, we used *in vivo* BrdU labeling in the FGF19 transgenic mice to assess hepatocellular proliferation. Labeled hepatocytes were predominantly perivenular (Figure 4B) whereas BrdU-labeled hepatocytes were rare in wild-type mice (Figure 4A). By 2 to 4 months of age the BrdU-labeling index of hepatocytes was eightfold higher in FGF19 transgenic females than age-matched wild-type females ($P = 0.00003$) and twofold to threefold higher in FGF19 transgenic males than age-matched wild-type males ($P = 0.040$) (Figure 4C). The labeling index is also increased twofold to threefold in 7- to 9-month-old female and male FGF19 transgenics relative to their respective controls ($P = 0.0000002$ and $P = 0.006$, respectively; Figure 4D). Together these data indicate hepatocellular proliferation precedes tumor development and that the proliferative fraction is predominantly pericentral hepatocytes.

To determine whether hepatocellular proliferation was because of acute effects of FGF19 *in vivo*, we injected the purified protein into nontransgenic female mice while infusing BrdU throughout a period of 6 days. Mice receiving rFGF19 protein had a significantly higher BrdU-labeling index than mice receiving vehicle alone ($P = 0.014$). Similar to results described above in FGF19 transgenic mice, rFGF19-injected mice have a threefold to fivefold increase in hepatocellular proliferation relative to vehicle-injected mice (Figure 4E).

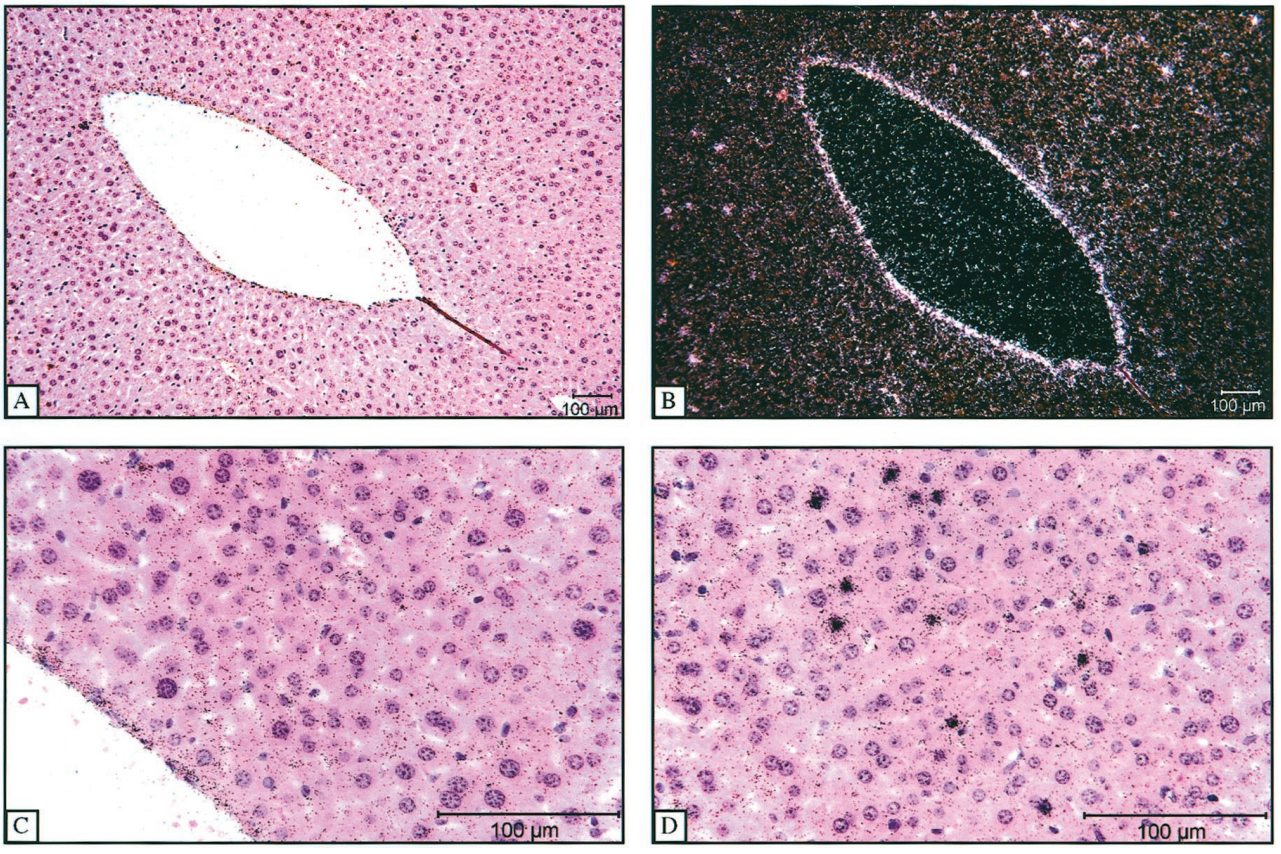

Figure 3. FGFR4 expression in murine liver. Bright-field (**A**) and dark-field (**B**) illumination of *in situ* hybridization with a murine FGFR4 riboprobe showing expression in perivenular and random hepatocytes. **C** and **D:** Higher magnification of bright-field demonstrating silver grains over random small hepatocytes. Original magnifications: ×100 (**A** and **B**); ×400 (**C** and **D**).

Pericentral Hepatocytes Give Rise to Neoplastic Foci

Glutamine synthetase is a marker for tracing hepatocellular lineage during preneoplastic and early neoplastic stages.[48] In the 10- to 12-month-old mice, 10 of 19 FGF19 transgenic mice had HCCs. All of the FGF19-induced tumors were strongly positive for glutamine synthetase by immunohistochemistry (Figure 5A). In contrast, liver from wild-type mice showed the expected pattern of staining one to three cell layers of pericentral hepatocytes (Figure 5, B and D). Foci of large dysplastic hepatocytes were also glutamine synthetase-positive (Figure 5C). Glutamine synthetase immunoreactivity of the neoplastic cells suggests they originated from the one to three cell layers of hepatocytes around the central veins that constitutively express glutamine synthetase.

AFP is an oncofetal protein expressed by neoplastic hepatocytes but not normal adult hepatocytes and is used as an indicator of neoplastic transformation in the liver.[39] Real-time reverse transcriptase-PCR showed hepatic AFP mRNA was elevated in FGF19 transgenic mice relative to wild types (Figure 6, A and B). At 2 to 4 months of age female transgenics had a 13-fold increase ($P = 0.01$) and male transgenics had an 18-fold increase ($P = 0.005$) in AFP expression relative to respective wild-type controls. The 7- to 9-month-old transgenic females had a fourfold increase ($P = 0.01$) and males had a threefold increase ($P = 0.03$) in AFP expression relative to respective wild-type controls. Subsequently, we evaluated AFP expression by *in situ* hybridization to determine which cells were expressing AFP before tumor formation. Consistent with our previous findings that indicated initial involvement of pericentral hepatocytes, AFP expression was demonstrated in hepatocytes adjacent to central veins (Figure 6, C and D). Neoplastic hepatocytes also consistently expressed AFP (Figure 6, E and F).

Expression of Growth Factors and Oncogenes in FGF19 Transgenic Mice

To investigate potential mechanisms of hepatocarcinogenesis, we evaluated expression of mRNA encoding TGF-α, hepatocyte growth factor, and c-*myc*. Overexpression of TGF-α alone[16,18] or in combination with c-*myc*[20] in the liver of transgenic mice leads to tumor development. In this study, real-time reverse transcriptase-PCR analysis at each time point did not demonstrate up-regulated expression of mRNA encoding TGF-α, hepatocyte growth factor, or c-*myc* in liver from MLC.FGF19 transgenic relative to age-matched wild-type mice (data not shown).

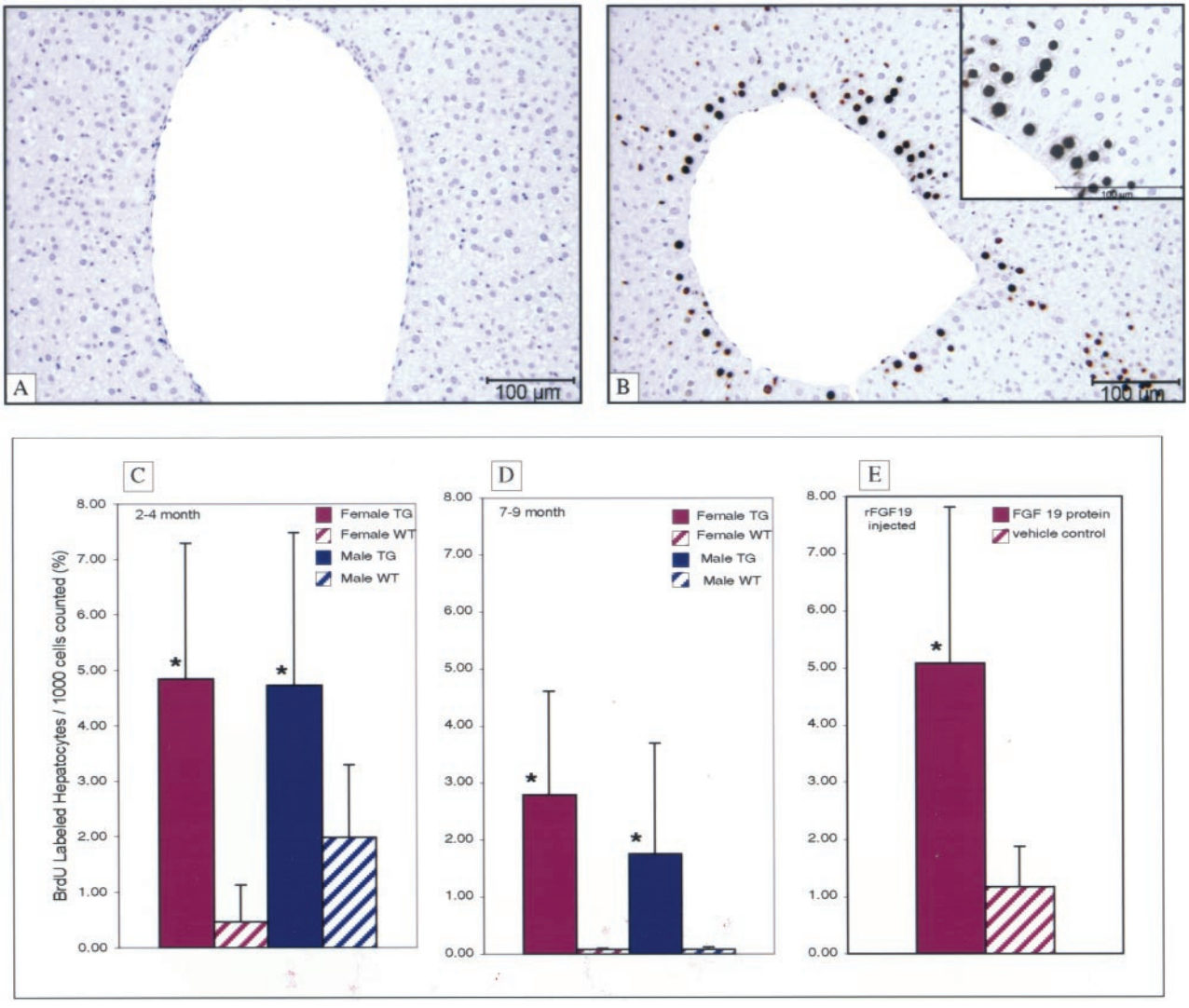

Figure 4. Increased proliferation of pericentral hepatocytes in FGF19 transgenics. Immunostaining for BrdU after a 5-day infusion by osmotic minipump of liver from a wild-type (**A**) and a FGF19 transgenic mouse (**B**). Morphometric analysis of BrdU-immunostained sections from FGF19 transgenics compared to wild-type mice: 2 to 4 months (**C**), 7 to 9 months (**D**), and FGF19-injected mice (**E**). The labeling index denotes the number of BrdU-positive hepatocytes divided by the total number of cells counted and indicated as a percentage. *, $P < 0.05$. Original magnifications: ×200 (**A** and **B**); ×600 (**inset** in **B**).

β-Catenin Activation and Somatic Mutations in MLC.FGF19 HCCs

To further evaluate the molecular pathogenesis of HCCs in FGF19 transgenic mice, we used immunohistochemical staining for β-catenin in addition to cloning and sequencing exon 2 of the *β-catenin* gene from tumor tissue. HCCs from nine different FGF19 transgenic mice were evaluated for immunoreactivity to β-catenin antibody. Four of the nine tumors (44%) had nuclear and cytoplasmic staining for β-catenin in neoplastic hepatocytes (Figure 7, A and B). All four tumors with β-catenin immunoreactivity were from female FGF19 transgenic mice in the 10- to 12-month age group. Cloning and sequencing hepatic DNA encoding exon 2 of β-catenin from tumor tissue that was immunohistochemistry-positive revealed point mutations that resulted in amino acid substitutions (Figure 7C). Overall, 16% of the clones contained mutations. A → G or G → A transitions were the most common mutations observed and involved codons 23, 34, 72, 76, and 80 (Table 3). Other transition mutations included C → T (codon 44), T → C (codon 70), and A → T (codon 56). Four of the clones from three different animals had mutations within the glycogen synthase kinase-3B (GSK-3B) phosphorylation domain at codon 34 and codon 44 (Figure 7, C and D). Of the four mutations within the phosphorylation domain, three resulted in substitution of an amino acid with a nonpolar side chain by an amino acid with a polar uncharged (Pro45Ser) or a polar charged (Gly34Glx) amino acid side chain. The fourth amino acid substitution within the phosphorylation domain retained the polar side chain but replaced a relatively small amino acid with a larger, space-occupying molecule (Gly34Ile). Seven other mutations resulted in amino acid substitutions in regions adjacent to the GSK-3B phosphorylation domain (Figure 7C). Of the mutations outside the phosphorylation domain, amino acid substitutions resulted in altered charge (Gln72Arg, Gln76Arg, Asx56Val), polarity

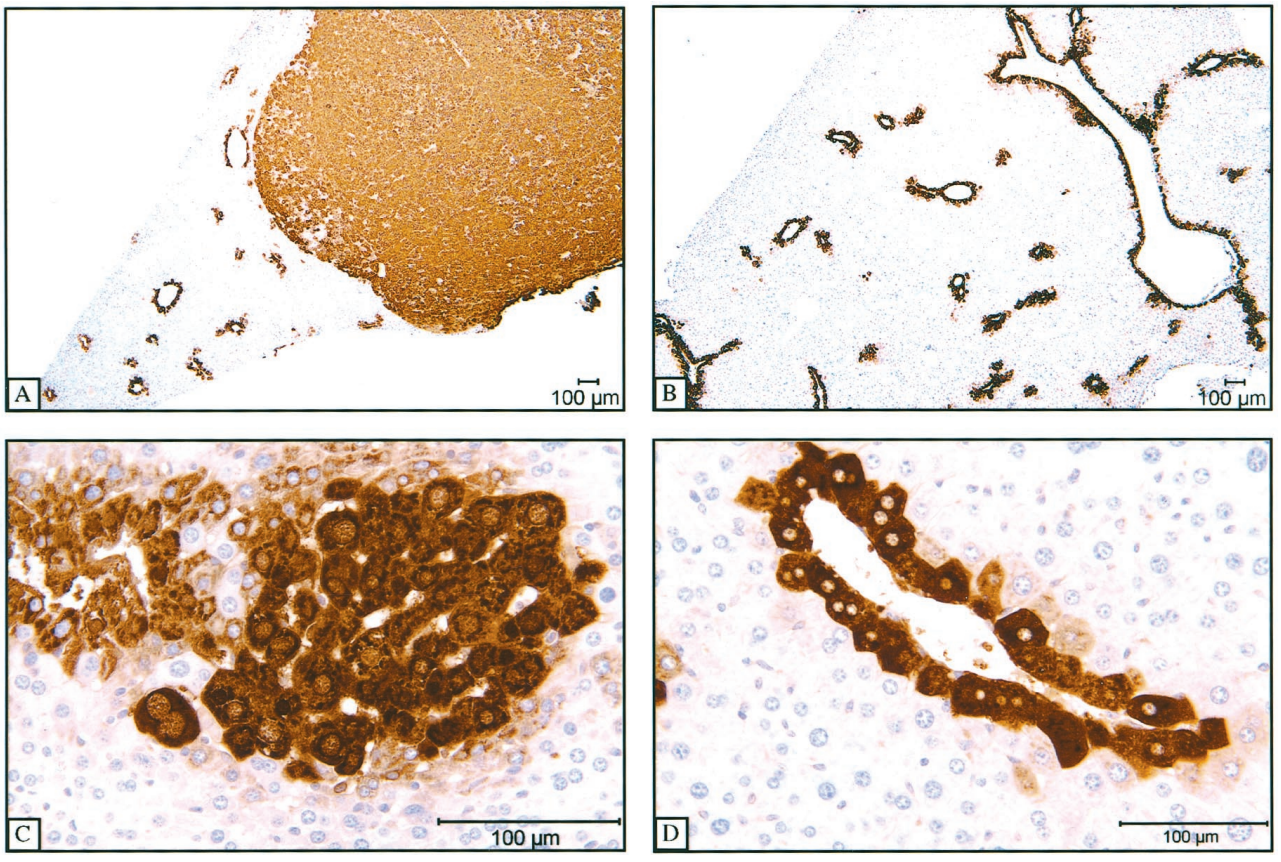

Figure 5. Glutamine synthetase immunoreactivity of dysplastic and neoplastic hepatocytes from FGF19 transgenics. **A:** Neoplastic cells are strongly glutamine synthetase-positive. **B:** Liver from a wild-type mouse showing normal perivenular glutamine synthetase immunostaining. **C:** Dysplastic hepatocytes are strongly glutamine synthetase-positive. **D:** Normal glutamine synthetase immunoreactivity of perivenular hepatocytes. Original magnifications: ×40 (**A** and **B**); ×400 (**C** and **D**).

(Ala80Ser, Ser23Gly), or molecular size (Phe70Leu). Mutations that affect GSK-3B phosphorylation of β-catenin prevent ubiquitination and degradation,[48,49] resulting in cytoplasmic accumulation and nuclear translocation of β-catenin, which accounts for the immunoreactivity observed in this study. Figure 7C shows the amino acid alignment of all mutant β-catenin clones compared to the wild-type sequence, depicting relative positions of amino acid substitutions and the GSK-3B phosphorylation domain.

Discussion

We have demonstrated that overexpression of FGF19 at an ectopic site (skeletal muscle) leads to liver dysplasia and HCCs in transgenic mice. Preneoplastic changes including AFP expression and increased hepatocellular proliferation have been confirmed in a second founder line to rule out insertional activation of a dominant oncogene resulting from integration of the transgene. In this study, FGF19 transgenic mice develop HCCs by 10 to 12 months of age with a higher incidence in female transgenics (Table 1). In contrast, transgenic mice overexpressing TGF-α in the liver under control of the metallothionein-I promoter have a higher incidence of tumors in males.[36] There is also a male predominance of HCC in humans in developed countries and worldwide.[51] Therefore, understanding the reason for the higher incidence of HCC in female FGF19 transgenic mice may help elucidate the pathogenesis of HCC in other species.

In the normal liver, hepatocytes are mitotically quiescent, remaining in the G_0 phase of the cell cycle. However, chemical carcinogens including phenobarbital and peroxisome proliferators[52,53] as well as overexpression of oncogenes in the liver[27] induce transient and/or sustained hepatocyte proliferation that precedes transformation. Although FGF19 is minimally mitogenic for fibroblasts *in vitro* relative to other FGF family members,[14] hepatocellular proliferation was significantly elevated in nontransgenic mice injected with FGF19 protein (Figure 4E) and in 2- to 4-month-old FGF19 transgenic mice (Figure 4C). These are data consistent with previous observations that constitutive hepatocyte proliferation precedes liver tumor development, with or without liver damage, in other transgenic mouse models.[27]

Mechanistic studies of hepatocarcinogens have identified specific morphological changes associated with unique molecular alterations.[54] For example, diethylnitrosamine induces pericentral foci of small dysplastic hepatocytes[55,56] and acts by ethylating nucleophilic sites in DNA.[57] Diethylnitrosamine-induced HCCs are also glutamine synthetase-positive suggesting that the neoplas-

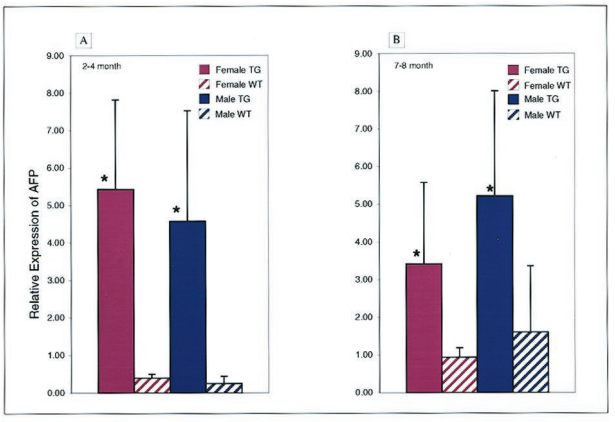

Figure 6. Expression of AFP by neoplastic and dysplastic hepatocytes. Increased expression of AFP mRNA in FGF19 transgenic liver compared to wild-type liver at 2 to 4 months of age (**A**) and 7 to 9 months of age (**B**). *, $P < 0.05$. Bright-field (**C**) and dark-field (**D**) illumination of *in situ* hybridization with AFP riboprobe showing expression of AFP by pericentral dysplastic hepatocytes (**arrows**). Bright-field (**E**) and dark-field (**F**) illumination of *in situ* hybridization with AFP riboprobe showing expression of AFP by neoplastic hepatocytes (**arrows**). Original magnifications, ×100.

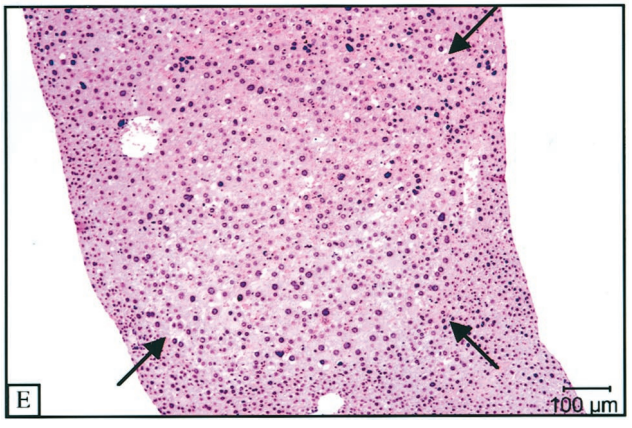

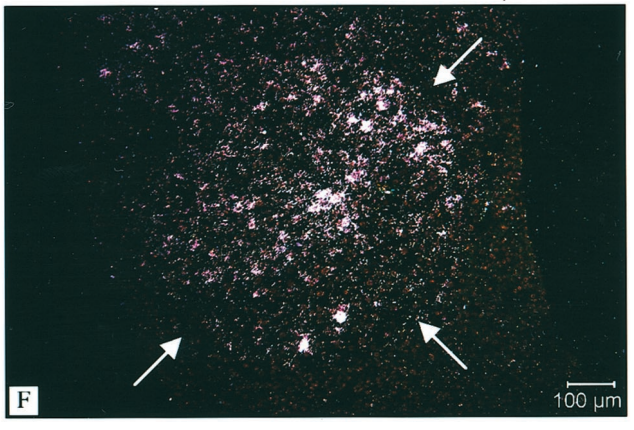

tic hepatocytes originated from the constitutive glutamine synthetase-positive population, pericentral hepatocytes.[58] Small dysplastic hepatocytes that oriented around the central veins were the predominant type of dysplasia that preceded neoplastic transformation in FGF19 transgenics (Figure 1C). Similarly, dysplastic and neoplastic foci in FGF19 transgenic mice were positive for glutamine synthetase (Figure 5). Selective involvement of pericentral hepatocytes may imply a potential pathogenesis of hepatocellular tumor formation such as DNA adduct formation that results from diethylnitrosamine. Alternatively, the pericentral hepatocytes that are highly metabolically active may be more susceptible to oxidative stress resulting in free radical formation, DNA damage, and subsequent tumor initiation. This concept has precedence in the TGF-α/c-*myc* double-transgenic mouse model of HCC in which an environment of oxidative stress is present before tumor formation[59] and treatment with vitamin E, a potent free-radical scavenging antioxidant, prevents progression to HCC.[60]

We have previously described an increased metabolic rate associated with decreased adiposity in FGF19 transgenic mice.[40] Whether HCC formation is an indirect effect of altered metabolism or a direct effect of FGF19 is unknown. Examples of mouse models in which altered metabolism leads to hepatocellular changes include liver dysplasia associated with loss of insulin signaling in hepatocytes of liver-specific insulin receptor knockout mice (LIRKO).[61] The authors hypothesized that hepatocellular dysplasia was because of oxidative stress, however, peri-

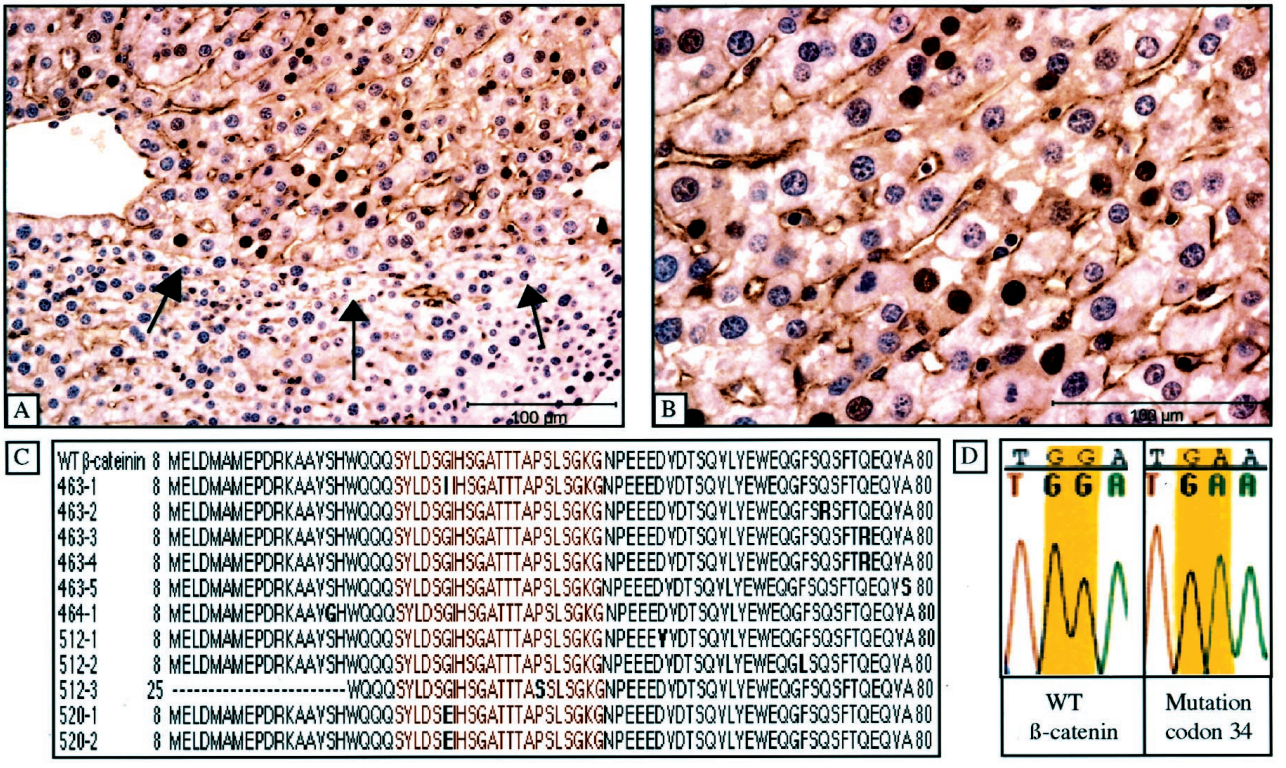

Figure 7. β-Catenin immunoreactivity of neoplastic hepatocytes from FGF19 transgenics. **A:** Strong nuclear staining of neoplastic cells compared with surrounding liver. **Arrows** mark the border of the tumor and adjacent normal liver. **B:** Neoplastic hepatocytes with nuclear immunoreactivity for β-catenin. **C:** Amino acid sequence alignment of the N-terminal region of β-catenin from wild-type (**top**) and mutant clones with amino acid substitutions (**bold**) in and adjacent to the GSK-3B phosphorylation domain (red). **D:** Sequencing data for DNA from normal liver and HCC with nucleotide substitutions at codon 34 (shaded). Original magnifications: ×200 (**A**); ×400 (**B**).

central hepatocytes were not preferentially affected in the LIRKO mice nor did the hepatocellular dysplasia described in their study progress to HCCs. Therefore, FGF19 may act directly as a tumor promotor instead of causing HCCs secondary to altered metabolism. Expression patterns of FGFR4, the receptor for FG19,[14] in murine liver (Figure 3) support the notion that FGF19 could directly activate hepatocytes.

Table 3. Nucleotide and Amino Acid Substitutions in β-Catenin Clones from FGF19 Transgenic HCCs that Have Nuclear Accumulation of β-Catenin Shown by Immunohistochemistry

Animal ID-clone number	Mutation	Codon	Amino acid change
463-1	(GG to AT)	34	Glycine to isoleucine*
463-2	(A to G)	72	Glutamine to arginine
463-3	(A to G)	76	Glutamine to arginine
463-4	(A to G)	76	Glutamine to arginine
463-5	(G to A)	80	Alanine to serine
464-1	(A to G)	23	Serine to glycine
512-1	(A to T)	56	Aspartic acid to valine
512-2	(T to C)	70	Phenylalanine to leucine
512-3	(C to T)	44	Proline to serine*
520-1	(GG to GA)	34	Glycine to glutamic acid*
520-2	(GG to GA)	34	Glycine to glutamic acid*
Total mutations	11/66 (16.6%)		

The animal identification followed by a hyphen and the clone number is indicated in the left column. The nucleotide substitution and affected codon are shown in the second and third columns, respectively. The amino acid change is shown on the right.

*The mutation was within the GSK-3B phosphorylation domain.

Because expression levels of growth factors and oncogenes were not altered in the FGF19 transgenic mice (data not shown), we determined whether mutations in tumor suppressors contributed to the hepatocarcinogenesis. HCCs in transgenic mouse models overexpressing c-*myc* or H-ras and human HCCs have activating somatic mutations within the β-catenin gene.[62–64] Mutations in β-catenin have also been identified in murine HCCs induced by diethylnitrosamine.[65] β-catenin is involved in cell adhesion and transmission of the proliferating signal of the Wingless/Wnt pathway.[66,67] Mutations in the gene encoding β-catenin typically affect the phosphorylation site thereby inhibiting GSK-3B phosphorylation of β-catenin that prevents ubiquitination and degradation.[49,50] Our results show that liver tumors from 44% (four of nine) of FGF19 transgenic mice had neoplastic cell nuclei that were immunoreactive with antibodies to β-catenin (Figure 7, A and B). Cloning and sequencing DNA from the FGF19 transgenic tumors clearly demonstrated point mutations leading to amino acid substitutions in and adjacent to the GSK-3B phosphorylation site of β-catenin (Figure 7C). Transition mutations resulting in amino acid substitutions in nine different codons were revealed (Table 3). A → G or G → A transitions were the most common mutations observed and involved codons 23 (Ser23Gly), 34 (Gly34Glu, Gly34Ile), 72 (Gln72Arg), 76

(Gln76Arg), and 80 (Ala80Ser). To our knowledge, only one of the mutations observed in the FGF19 transgenic HCCs, Gly34Glu, has been previously described in murine HCC.[64]

β-Catenin mutation frequency is variable in different transgenic mouse models of liver cancer. Previous studies demonstrate β-catenin mutation frequencies of 5 to 12% in HCCs from c-*myc*, c-*myc*/TGF-α, and c-*myc*/TGF-β1 transgenic mice in which transgene expression is driven in the liver by the albumin promoter.[63] However, a higher β-catenin mutation frequency, 40 to 55%, occurs in HCCs from transgenic mice overexpressing H-ras or c-*myc* under control of the L-type pyruvate kinase (L-PK) promoter, and c-*myc* under control of the woodchuck hepatitis virus promoter.[64] β-catenin nuclear translocation in 44% of the FGF19 HCCs, with β-catenin mutations identified by sequencing DNA from these tumors, is in accordance with the β-catenin mutation frequency from the latter group of L-PK/H-ras, L-PK/c-*myc*, and woodchuck hepatitis virus/c-*myc* transgenic mouse models. The variability of β-catenin mutation frequency may be attributable to the different background strains as has been suggested,[63] or indicative of specific molecular mechanisms of hepatocellular transformation.

Taken together, these data suggest a previously unknown role for FGF19 in hepatocarcinogenesis. Hepatocellular proliferation in young transgenic mice and rFGF19 protein-injected mice implies FGF19 may directly affect hepatocytes. Expression of the receptor for FGF19, FGFR4, in murine liver supports this hypothesis. Moreover, our data implicate the Wingless/Wnt pathway in the molecular pathogenesis of HCCs in FGF19 transgenic mice. Further studies may define novel roles for FGF19 in carcinogenesis.

Acknowledgments

We thank Marjie Van Hoy and Erik Pegg for necropsy assistance; Robin E. Taylor, Shawn Salesky, Patti Tobin, and Julio Ramirez for paraffin embedding and sectioning; Sharon Erickson for generating the mice; and Austin Gurney, Ellen Filvaroff, Joseph Beyer, and Frank Peale for helpful discussions.

References

1. Ornitz DM, Itoh N: Fibroblast growth factors. Genome Biol 2001, 2:3005.1–3005.12
2. Marsh SK, Bansal GS, Zammit C, Barnard R, Coope R, Roberts-Clarke D, Gomm JJ, Coombes RC, Johnston CL: Increased expression of fibroblast growth factor 8 in human breast cancer. Oncogene 1999, 18:1053–1060
3. Mattila MM, Ruohola JK, Valve EM, Tasanen MJ, Seppanen JA, Harkonen PL: FGF-8b increases angiogenic capacity and tumor growth of androgen-regulated S115 breast cancer cells. Oncogene 2001, 20:2791–2804
4. Ruohola JK, Viitanen TP, Valve EM, Seppanen JA, Loponen NT, Keskitalo JJ, Lakkakorpi PT, Harkonen PL: Enhanced invasion and tumor growth of fibroblast growth factor 8b-overexpressing MCF-7 human breast cancer cells. Cancer Res 2001, 61:4229–4237
5. Valve EM, Nevalainen MT, Nurmi MJ, Laato MK, Martikainen PM, Harkonen PL: Increased expression of FGF-8 isoforms and FGF receptors in human premalignant prostatic intraepithelial neoplasia lesions and prostate cancer. Lab Invest 2001, 81:815–826
6. Dorkin TJ, Robinson MC, Marsh C, Bjartell A, Neal DE, Leung HY: FGF8 over-expression in prostate cancer is associated with decreased patient survival and persists in androgen independent disease. Oncogene 1999, 18:2755–2761
7. Dorkin TJ, Robinson MC, Marsh C, Neal DE, Leung HY: aFGF immunoreactivity in prostate cancer and its co-localization with bFGF and FGF8. J Pathol 1999, 189:564–569
8. Krejci P, Dvorakova D, Krahulcova E, Pachernik J, Mayer J, Hampl A, Dvorak P: FGF-2 abnormalities in B cell chronic lymphocytic and chronic myeloid leukemias. Leukemia 2001, 15:228–237
9. Daphna-Iken D, Shankar DB, Lawshe A, Ornitz DM, Shackleford GM, MacArthur CA: MMTV-Fgf8 transgenic mice develop mammary and salivary gland neoplasia and ovarian stromal hyperplasia. Oncogene 1998, 17:2711–2717
10. Clark JC, Tichelaar JW, Wert SE, Itoh N, Perl AK, Stahlman MT, Whitsett JA: FGF-10 disrupts lung morphogenesis and causes pulmonary adenomas in vivo. Am J Physiol 2001, 280:L705–L715
11. La Rosa S, Sessa F, Colombo L, Tibiletti MG, Furlan D, Capella C: Expression of acidic fibroblast growth factor (aFGF) and fibroblast growth factor receptor 4 (FGFR4) in breast fibroadenomas. J Clin Pathol 2001, 54:37–41
12. Chesi M, Brents LA, Ely SA, Bais C, Robbiani DF, Mesri EA, Kuehl WM, Bergsagel PL: Activated fibroblast growth factor receptor 3 is an oncogene that contributes to tumor progression in multiple myeloma. Blood 2001, 97:729–736
13. Jang JH, Shin KH, Park JG: Mutations in fibroblast growth factor receptor 2 and fibroblast growth factor receptor 3 genes associated with human gastric and colorectal cancers. Cancer Res 2001, 61: 3541–3543
14. Xie MH, Holcomb I, Deuel B, Dowd P, Huang A, Vagts A, Foster J, Liang J, Brush J, Gu Q, Hillan K, Goddard A, Gurney AL: FGF-19, a novel fibroblast growth factor with unique specificity for FGFR4. Cytokine 1999, 11:729–735
15. Murray CJ, Lopez AD: Mortality by cause for eight regions of the world: global burden of disease study. Lancet 1997, 349:1269–1276
16. Jhappan C, Stahle C, Harkins RN, Fausto N, Smith GH, Merlino GT: TGF alpha overexpression in transgenic mice induces liver neoplasia and abnormal development of the mammary gland and pancreas. Cell 1990, 61:1137–1146
17. Sandgren EP, Luetteke NC, Qiu TH, Palmiter RD, Brinster RL, Lee DC: Transforming growth factor alpha dramatically enhances oncogene-induced carcinogenesis in transgenic mouse pancreas and liver. Mol Cell Biol 1993, 13:320–330
18. Sandgren EP, Quaife CJ, Pinkert CA, Palmiter RD, Brinster RL: Oncogene-induced liver neoplasia in transgenic mice. Oncogene 1989, 4:715–724
19. Lee GH, Merlino G, Fausto N: Development of liver tumors in transforming growth factor alpha transgenic mice. Cancer Res 1992, 52:5162–5170
20. Murakami H, Sanderson ND, Nagy P, Marino PA, Merlino G, Thorgeirsson SS: Transgenic mouse model for synergistic effects of nuclear oncogenes and growth factors in tumorigenesis: interaction of c-myc and transforming growth factor alpha in hepatic oncogenesis. Cancer Res 1993, 53:1719–1723
21. Saitoh A, Kimura M, Takahashi R, Yokoyama M, Nomura T, Izawa M, Sekiya T, Nishimura S, Katsuki M: Most tumors in transgenic mice with human c-Ha-ras gene contained somatically activated transgenes. Oncogene 1990, 5:1195–2000
22. Toshkov I, Chisari FV, Bannasch P: Hepatic preneoplasia in hepatitis B virus transgenic mice. Hepatology 1994, 20:1162–1172
23. Koike K, Moriya K, Iino S, Yotsuyanagi H, Endo Y, Miyamura T, Kurokawa K: High-level expression of hepatitis B virus HBx gene and hepatocarcinogenesis in transgenic mice. Hepatology 1994, 19:810–819
24. Sepulveda AR, Finegold MJ, Smith B, Slagle BL, DeMayo JL, Shen RF, Woo SL, Butel JS: Development of a transgenic mouse system for the analysis of stages in liver carcinogenesis using tissue-specific expression of SV40 large T-antigen controlled by regulatory elements of the human alpha-1-antitrypsin gene. Cancer Res 1989, 49:6108–6117
25. Schirmacher P, Held WA, Yang D, Biempica L, Rogler CE: Selective amplification of periportal transitional cells precedes formation of

hepatocellular carcinoma in SV40 large tag transgenic mice. Am J Pathol 1991, 139:231–241
26. Fausto N: Liver regeneration. J Hepatol 2000, 32:19–31
27. Fausto N: Mouse liver tumorigenesis: models, mechanisms, and relevance to human disease. Semin Liver Dis 1999, 19:243–252
28. Chisari FV, Klopchin K, Moriyama T, Pasquinelli C, Dunsford HA, Sell S, Pinkert CA, Brinster RL, Palmiter RD: Molecular pathogenesis of hepatocellular carcinoma in hepatitis B virus transgenic mice. Cell 1989, 59:1145–1156
29. Dunsford HA, Sell S, Chisari FV: Hepatocarcinogenesis due to chronic liver cell injury in hepatitis B virus transgenic mice. Cancer Res 1990, 50:3400–3407
30. Smit JJ, Schinkel AH, Oude Elferink RP, Groen AK, Wagenaar E, van Deemter L, Mol CA, Ottenhoff R, van der Lugt NM, van Roon MA: Homozygous disruption of the murine mdr2 P-glycoprotein gene leads to a complete absence of phospholipid from bile and to liver disease. Cell 1993, 75:451–462
31. Fan CY, Pan J, Usuda N, Yeldandi AV, Rao MS, Reddy JK: Steatohepatitis, spontaneous peroxisome proliferation and liver tumors in mice lacking peroxisomal fatty acyl-CoA oxidase. Implications for peroxisome proliferator-activated receptor alpha natural ligand metabolism. J Biol Chem 1998, 273:15639–15645
32. Hsu T, Moroy T, Etiemble J, Louise A, Trepo C, Tiollais P, Buendia MA: Activation of c-myc by woodchuck hepatitis virus insertion in hepatocellular carcinoma. Cell 1988, 55:627–635
33. Hsu TY, Fourel G, Etiemble J, Tiollais P, Buendia MA: Integration of hepatitis virus DNA near c-myc in woodchuck hepatocellular carcinoma. Gastroenterol Jpn 1990, 25:43–48
34. Fourel G, Trepo C, Bougueleret L, Henglein B, Ponzetto A, Tiollais P, Buendia MA: Frequent activation of N-myc genes by hepadnavirus insertion in woodchuck liver tumours. Nature 1990, 347:294–298
35. Takagi H, Sharp R, Hammermeister C, Goodrow T, Bradley MO, Fausto N, Merlino G: Molecular and genetic analysis of liver oncogenesis in transforming growth factor alpha transgenic mice. Cancer Res 1992, 52:5171–5177
36. Santoni-Rugiu E, Nagy P, Jensen MR, Factor VM, Thorgeirsson SS: Evolution of neoplastic development in the liver of transgenic mice co-expressing c-myc and transforming growth factor-alpha. Am J Pathol 1996, 149:407–428
37. Sandgren EP, Merlino G: Hepatocarcinogenesis in transgenic mice. Prog Clin Biol Res 1995, 391:213–222
38. Araki K, Hino O, Miyazaki J, Yamamura K: Development of two types of hepatocellular carcinoma in transgenic mice carrying the SV40 large T-antigen gene. Carcinogenesis 1991, 12:2059–2062
39. Peng SY, Lai PL, Chu JS, Lee PH, Tsung PT, Chen DS, Hsu HC: Expression and hypomethylation of alpha-fetoprotein gene in unicentric and multicentric human hepatocellular carcinomas. Hepatology 1993, 17:35–41
40. Tomlinson E, Fu L, John L, Hultgren B, Huang X, Renz M, Stephan JP, Tsai SP, Powell-Braxton L, French D, Stewart TA: Transgenic mice expressing human fibroblast growth factor-19 display increased metabolic rate and decreased adiposity. Endocrinology 2002, in press
41. Shani M: Tissue-specific expression of rat myosin light-chain 2 gene in transgenic mice. Nature 1985, 314:283–286
42. Stewart TA, Clift S, Pitts-Meek S, Martin L, Terrell TG, Liggitt D, Oakley H: An evaluation of the functions of the 22-kilodalton (kDa), the 20-kDa, and the N-terminal polypeptide forms of human growth hormone using transgenic mice. Endocrinology 1992, 130:405–414
43. Lu L, Gillet N: An optimized protocol for in situ hybridization using PCR-generated 33P-labeled riboprobes. Cell Vis 1994, 1:169–176
44. Holcomb IN, Kabakoff RC, Chan B, Baker TW, Gurney A, Henzel W, Nelson C, Lowman HB, Wright BD, Skelton NJ, Frantz GD, Tumas DB, Peale Jr FV, Shelton DL, Hebert CC: FIZZ1, a novel cysteine-rich secreted protein associated with pulmonary inflammation, defines a new gene family. EMBO J 2000, 19:4046–4055
45. Korhonen J, Partanen J, Alitalo K: Expression of FGFR-4 mRNA in developing mouse tissues. Int J Dev Biol 1992, 36:323–329
46. Stark KL, McMahon JA, McMahon AP: FGFR-4, a new member of the fibroblast growth factor receptor family, expressed in the definitive endoderm and skeletal muscle lineages of the mouse. Development 1991, 113:641–651
47. Kan M, Wu X, Wang F, McKeehan WL: Specificity for fibroblast growth factors determined by heparan sulfate in a binary complex with the receptor kinase. J Biol Chem 1999, 274:15947–15952
48. Gebhardt R, Williams GM: Glutamine synthetase and hepatocarcinogenesis. Carcinogenesis 1995, 16:1673–1681
49. Aberle H, Bauer A, Stappert J, Kispert A, Kemler R: Beta-catenin is a target for the ubiquitin-proteasome pathway. EMBO J 1997, 16:3797–3804
50. Yost C, Torres M, Miller JR, Huang E, Kimelman D, Moon RT: The axis-inducing activity, stability, and subcellular distribution of beta-catenin is regulated in Xenopus embryos by glycogen synthase kinase 3. Genes Dev 1996, 10:1443–1454
51. Parkin DM, Pisani P, Ferlay J: Estimates of the worldwide incidence of 25 major cancers in 1990. Int J Cancer 1999, 80:827–841
52. Cunningham ML: Role of increased DNA replication in the carcinogenic risk of nonmutagenic chemical carcinogens. Mutat Res 1996, 365:59–69
53. Swenberg JA, Maronpot RR: Chemically induced cell proliferation as a criterion in selecting doses for long-term bioassays. Prog Clin Biol Res 1991, 369:245–251
54. Harada T, Enomoto A, Boorman GA, Maronpot RR: Liver and Gallbladder. Pathology of the Mouse. Edited by RR Maronpot, GA Boorman, BW Gaul. Vienna, Cache River Press, 1999, pp 119–183
55. Koen H, Pugh TD, Goldfarb S: Centrilobular distribution of diethylnitrosamine-induced hepatocellular foci in the mouse. Lab Invest 1983, 49:78–81
56. Goldfarb S, Pugh TD, Koen H, He YZ: Preneoplastic and neoplastic progression during hepatocarcinogenesis in mice injected with diethylnitrosamine in infancy. Environ Health Perspect 1983, 50:149–161
57. Beranek DT: Distribution of methyl and ethyl adducts following alkylation with monofunctional alkylating agents. Mutat Res 1990, 231: 11–30
58. Gebhardt R, Tanaka T, Williams GM: Glutamine synthetase heterogeneous expression as a marker for the cellular lineage of preneoplastic and neoplastic liver populations. Carcinogenesis 1989, 10: 1917–1923
59. Factor VM, Kiss A, Woitach JT, Wirth PJ, Thorgeirsson SS: Disruption of redox homeostasis in the transforming growth factor-alpha/c-myc transgenic mouse model of accelerated hepatocarcinogenesis. J Biol Chem 1998, 273:15846–15853
60. Factor VM, Laskowska D, Jensen MR, Woitach JT, Popescu NC, Thorgeirsson SS: Vitamin E reduces chromosomal damage and inhibits hepatic tumor formation in a transgenic mouse model. Proc Natl Acad Sci USA 2000, 97:2196–2201
61. Michael MD, Kulkarni RN, Postic C, Previs SF, Shulman GI, Magnuson MA, Kahn CR: Loss of insulin signaling in hepatocytes leads to severe insulin resistance and progressive hepatic dysfunction. Mol Cell 2000, 6:87–97
62. Terris B, Pineau P, Bregeaud L, Valla D, Belghiti J, Tiollais P, Degott C, Dejean A: Close correlation between beta-catenin gene alterations and nuclear accumulation of the protein in human hepatocellular carcinomas. Oncogene 1999, 18:6583–6588
63. Calvisi DF, Factor VM, Loi R, Thorgeirsson SS: Activation of beta-catenin during hepatocarcinogenesis in transgenic mouse models: relationship to phenotype and tumor grade. Cancer Res 2001, 61: 2085–2091
64. de La Coste A, Romagnolo B, Billuart P, Renard CA, Buendia MA, Soubrane O, Fabre M, Chelly J, Beldjord C, Kahn A, Perret C: Somatic mutations of the beta-catenin gene are frequent in mouse and human hepatocellular carcinomas. Proc Natl Acad Sci USA 1998, 95:8847–8851
65. Ogawa K, Yamada Y, Kishibe K, Ishizaki K, Tokusashi Y: Beta-catenin mutations are frequent in hepatocellular carcinomas but absent in adenomas induced by diethylnitrosamine in B6C3F1 mice. Cancer Res 1999, 59:1830–1833
66. Miller JR, Moon RT: Signal transduction through beta-catenin and specification of cell fate during embryogenesis. Genes Dev 1996, 10:2527–2539
67. Barth AI, Nathke IS, Nelson WJ: Cadherins, catenins and APC protein: interplay between cytoskeletal complexes and signaling pathways. Curr Opin Cell Biol 1997, 9:683–690